Transport of broadband radiation through a nonlinear dispersive medium

James S. Cohen and O. P. Judd
Los Alamos National Laboratory, University of California, Los Alamos, New Mexico 87545
(Received 21 October 1982)

Analytical and numerical solutions are presented to elucidate the important physical aspects of the incoherent nonlinear interaction and propagation of high-intensity radiation in an absorbing (or amplifying) medium. The properties of radiation-driven one-dimensional density discontinuities or wave fronts are examined for monochromatic and broadband radiation sources, and for a nonlinear absorbing medium characterized by a spectral absorption cross section that is square, Gaussian, or Lorentzian. The effect of the angular distribution of the radiation source is considered in detail. The results of the analysis show that the propagation behavior of the radiation-driven wave front depends strongly on the spectral dependence of the absorption cross section. The wave front propagates with a constant shape and at a constant velocity v_b only for monochromatic radiation or a square absorption cross section. For a Lorentzian, $v_b \sim x^{1/2}$ at large values of the propagation distance x. The absorption of intense radiation in a medium generally causes local heating, which can introduce hydrodynamic disturbances that propagate behind, along with, or ahead of the radiation-driven wave front. Conditions are derived for the amount of heat addition that is required to produce these disturbances for a given velocity of the wave front.

I. INTRODUCTION

We consider in this work the nonlinear interaction and propagation of high-intensity radiation in an absorbing medium. We will emphasize the situation in which the medium is optically thick and limit the analysis to one-dimensional propagation. Coherent interactions between the radiation field and the medium will be neglected. This problem has been addressed by a number of investigators for the case of monochromatic radiation. For a saturating two-level system, the solutions can be written in closed analytic form.[1-3] Under certain conditions, they are also valid for a medium with gain such as lasers. The results of these analyses show that for sufficiently high intensity, a radiation driven density discontinuity or wave front is formed that propagates into the medium. The medium is transparent behind the front and opaque ahead of the front. The wave front maintains a constant shape and propagates with a constant velocity v_b given by ϕ_0/n_0, where ϕ_0 is the photon intensity of the radiation source and n_0 is the number density of saturable absorbers in the medium.

For several applications of interest, the radiation source may emit a broadband spectrum, for example, a blackbody emitter. If the absorption spectrum of the medium is narrow compared to the emission spectrum of the source, the behavior of the propagation of the radiation wave is changed significantly and depends strongly on the detailed spectral properties of the absorber and radiation field. This particular regime has been addressed by only a few investigators[4-6] for which the published results appear to be conflicting and/or ambiguous. It is this specific regime that we wish to address in this work.

Nonlinear radiation transport is encountered in a number of scientific areas. Transport of monochromatic radiation has been studied extensively in the fields of lasers and saturable absorbers,[1-3] propagation through the atmosphere,[7] nonlinear crystals, and laser induced chemistry.[8-11] The transport of intense *broadband* radiation has important implications in astrophysics,[12] fireballs produced by a nuclear explosion in the atmosphere,[13] and optical pumping of lasers.[14-20] Because of the specific applications, some of these analyses tend to obscure the generic aspects of the phenomena resulting from intense light sources. This paper will address the general aspects of broadband radiation transport in a nonlinear medium. We will consider in detail the specific example of optical pumping of an iodine laser in a separate paper.

II. NONLINEAR RADIATION TRANSPORT EQUATIONS

Although we consider a one-dimensional geometry, the transport of radiation is fundamental-

ly a three-dimensional process that involves the angular distribution of the radiation field. The equation for radiation transport in a linear medium and the related field quantities are reviewed in the Appendix. Most of these equations can be carried over directly to the nonlinear medium.

The radiation field is characterized by a scalar photon spectral intensity function $I_\nu(\vec{r},t,\hat{\Omega})$, where I_ν is the number of photons at time t in a frequency range ν to $\nu+d\nu$ passing per unit of time through a unit area located at position $\vec{r}$ and contained within a solid angle $d\Omega$ in the direction of a unit propagation vector $\hat{\Omega}$. We can now use the general formalism developed in the Appendix and specialize to one-dimensional propagation along a coordinate x. The spectral intensity can then be written in the functional form $I_\nu(x,t,\theta)$, where θ is the angle between $\hat{\Omega}$ and the propagation direction. Neglecting the finite propagation time of the radiation, the radiation transport equation can be expressed in the form

$$\cos\theta\frac{\partial I_\nu}{\partial x}=-\kappa_\nu(x,t)(I_\nu-I_{\nu e}) , \tag{1}$$

where $\kappa_\nu(x,t)$ is the net nonlinear absorption coefficient of the medium and $I_{\nu e}$ is the value of I_ν that results from spontaneous emission in the medium. The expression for κ_ν also includes the effects of stimulated emission. Consequently, κ_ν depends on the population densities for both the lower and upper state of the absorbing transition. Since the population densities can depend on I_ν, in general, κ_ν is an implicit nonlinear function of I_ν. In order to evaluate this nonlinear dependence, it is necessary to consider the details of the interaction of the radiation with the medium.

In the simplest approximation, we consider the atomic medium to be a nondegenerate two-level system. The population densities of the upper and lower levels are given by $n_u(x,t)$ and $n_l(x,t)$, respectively. Within a rate-equation description, the level densities satisfy the equations

$$\frac{\partial n_u}{\partial t}=R_u-\gamma_u n_u+(n_l-n_u)\langle\sigma_\nu I_\nu\rangle \tag{2}$$

and

$$\frac{\partial n_l}{\partial t}=R_l-\gamma_l n_l-(n_l-n_u)\langle\sigma_\nu I_\nu\rangle , \tag{3}$$

where

$$\langle\sigma_\nu I_\nu\rangle=\int_{4\pi}\int_0^\infty \sigma_\nu I_\nu\, d\nu\, d\Omega , \tag{4}$$

σ_ν is the frequency dependent absorption (or stimulated-emission) cross section, R is a net pump rate into the level from all sources other than stimulated processes, and γ is a net loss rate of the level. In general, σ_ν, R, and γ are determined by the chemical kinetics of the medium. Although not indicated explicitly, σ_ν may also be an implicit function of space and time. The net loss of photons from the radiation field (absorption minus stimulated emission) for each spectral component is given by the term $(n_l-n_u)\sigma_\nu I_\nu\equiv\kappa_\nu I_\nu$. Spontaneous emission results from the term involving γ_u.

If we neglect the effects of spontaneous emission, the radiation transport equation for each spectral component can be written in the form

$$\cos\theta\frac{\partial I_\nu}{\partial x}=-(n_l-n_u)\sigma_\nu I_\nu . \tag{5}$$

The neglect of the spontaneous-emission term is a good approximation in the applications that will be discussed.

Equations (2)–(5) constitute a closed set of nonlinear integro–partial-differential equations that describe the nonlinear physical behavior of an absorbing or amplifying medium. We now consider specific examples that yield simplified analytic solutions.

A. Isolated two-level system

In this case we assume that the pump and decay rates of each level are slow compared to the time scale for the interaction with the radiation field. Under these conditions we let $R\to 0$ and $\gamma\to 0$. Subtracting (2) from (3) and defining $\Delta n=(n_l-n_u)$ we obtain the equations

$$\cos\theta\frac{\partial I_\nu}{\partial x}=-\Delta n\sigma_\nu I_\nu \tag{6}$$

and

$$\frac{\partial\Delta n}{\partial t}=-2\Delta n\langle\sigma_\nu I_\nu\rangle . \tag{7}$$

The factor of 2 in Eq. (7) arises because the system is composed of two levels that are nondegenerate.

B. Steady-state approximation

We here assume the opposite limit to that in Sec. II A and let $(\partial/\partial t)\to 0$. Then

$$\cos\theta\frac{\partial I_\nu}{\partial x}=-\frac{(\Delta n_0)\sigma_\nu I_\nu}{1+\left[\dfrac{\gamma_u+\gamma_l}{\gamma_u\gamma_l}\right]\langle\sigma_\nu I_\nu\rangle} , \tag{8}$$

where $\Delta n_0=-(R_u/\gamma_u-R_l/\gamma_l)$ is the initial population difference in the system.

C. Photodissociation or photoionization

In photodissociation, molecules in the ground electronic state make a transition to an upper electronic state that undergoes dissociation on a short-time scale. Under these conditions, to good approximation $n_u \approx 0$. We further assume that $\gamma_l = 0$, but that recombination of the photofragments, which is a source or pumping term for the lower state, may occur. We assume a simple binary process in which $R_l = k_r n_l^2$. The equation describing the dissociation is then of the form

$$\frac{\partial n_l}{\partial t} = -n_l \langle \sigma_\nu I_\nu \rangle + k_r (n_{l0} - n_l)^2 . \tag{9}$$

An equation of this form is also obtained for photoionization processes.

III. SOLUTIONS OF THE NONLINEAR TRANSPORT EQUATIONS

From the above examples we find a large class of nonlinear radiation transport problems that can be described by equations of the general form

$$\cos\theta \frac{\partial I_\nu}{\partial x} = -n \sigma_\nu I_\nu \tag{10}$$

and

$$\frac{\partial n}{\partial t} = -n \langle \sigma_\nu I_\nu \rangle , \tag{11}$$

where $\langle \sigma_\nu I_\nu \rangle$ is given by Eq. (4). These equations can easily be converted into a single integro–partial-differential equation of the form

$$\frac{\partial n}{\partial t} = -n \int_{4\pi} \int_0^\infty \sigma_\nu I_\nu(0,t,\theta) \times \exp\left[- \int_0^x \frac{\sigma_\nu n(x',t)}{\cos\theta} dx' \right] \times d\nu \, d\Omega . \tag{12}$$

This form of the equations clearly indicates that while the final result depends on x and t, the character of the solution also depends strongly on θ and ν. In order to explore this behavior we now consider solutions for several special cases.

A. Collimated radiation in a nonlinear absorber

For this situation we assume I_ν is strongly peaked in the positive x direction. Since for normal collimated radiation the main contribution (at all x and t neglecting scattering) occurs for $\cos\theta = 1$, we can integrate Eq. (10) over $d\Omega$. In this case the radiation flux, Eq. (A3), is

$$S_\nu \approx \int_{4\pi} I_\nu d\Omega , \tag{13}$$

and Eqs. (10) and (11) become

$$\frac{\partial S_\nu}{\partial x} = -n \sigma_\nu S_\nu \tag{14}$$

and

$$\frac{\partial n}{\partial t} = -n \int_0^\infty \sigma_\nu S_\nu d\nu . \tag{15}$$

We consider a radiation source at $x = 0$, and a cross section of the form $\sigma_\nu = \sigma_0 g(\nu)$, where σ_0 is the maximum value of the cross section and $g(\nu)$ characterizes the spectral dependence of the absorption. A formal solution of Eq. (14) can be written in the form

$$S_\nu(x,t) = S_\nu(0,t) \exp\left[- \int_0^x n(x',t) \sigma_0 g(\nu) dx' \right] . \tag{16}$$

It is convenient to define an average center frequency normalized optical thickness τ by

$$\tau(x,t) = \sigma_0 \int_0^x n(x',t) dx' . \tag{17}$$

If we also assume a spatially uniform medium at $t = 0$ with density n_0, we can define the optical depth $\zeta = (n_0 \sigma_0)^{-1}$ for which $\tau(x,0) = x/\zeta = n_0 \sigma_0 x$. Substituting Eqs. (14), (16), and (17) into Eq. (15) gives the result

$$\frac{\partial n}{\partial t} = \frac{\partial}{\partial x} \int_0^\infty S_\nu(0,t) \exp[-\tau g(\nu)] d\nu . \tag{18}$$

From Eqs. (17) and (18) we obtain the set

$$\frac{\partial \tau}{\partial t} = -\sigma_0 \int_0^\infty S_\nu(0,t) \{ 1 - \exp[-\tau g(\nu)] \} d\nu \tag{19}$$

and

$$\frac{\partial \tau}{\partial x} = \sigma_0 n(x,t) . \tag{20}$$

For any $g(\nu)$, the integral in Eq. (19) can be evaluated (numerically if required) as a function of τ. The equation can then be solved to obtain $\tau(x,t)$. Substitution into Eq. (20) then gives $n(x,t)$.

A square cross section is defined by the functional form, $g(\nu) = 1$ for $\nu_0 - (\Delta\nu/2) < \nu < \nu_0 + (\Delta\nu/2)$ and zero otherwise. Numerical results for a square cross section (or monochromatic radiation), a Gaussian cross section, and a Lorentzian cross section are shown in Figs. 1(a)–1(c), respectively. The fraction bleached,

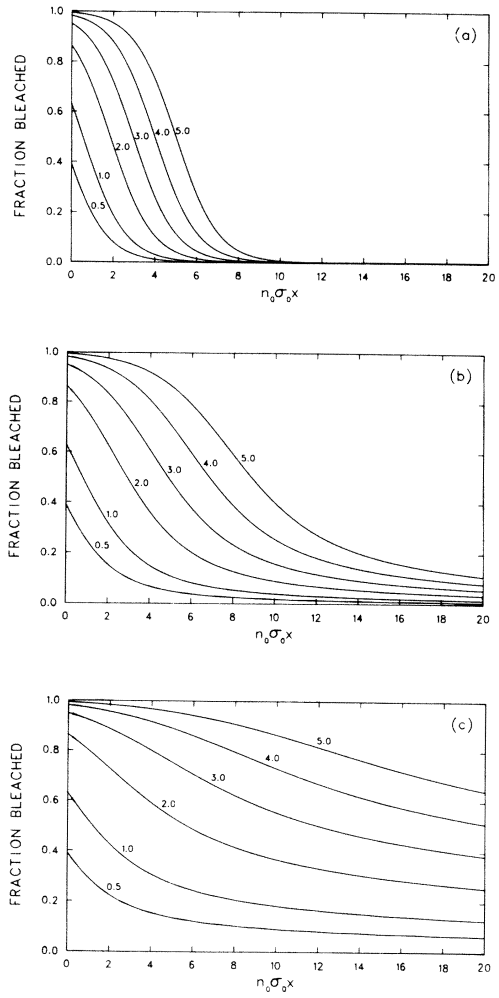

FIG. 1. "Bleaching waves" propagated by normal collimated radiation with (a) a square absorption cross section (or monochromatic radiation), (b) a Gaussian absorption cross section, and (c) a Lorentzian absorption cross section. Fraction bleached f_b is shown as a function of the dimensionless variable $n_0\sigma_0 x$ in each case at six different times corresponding to the designated values of Υ_0 [defined by Eq. (22)].

$$f_b \equiv 1 - n(x,t)/n_0 \ , \tag{21}$$

is shown as a function of $n_0\sigma_0 x$ at several propagation times. These times were chosen such that the energy absorbed by an optically thin target is the same for each cross section, i.e., the curves are labeled by

$$\Upsilon_0 = \int_0^t \langle \sigma_\nu I_\nu \rangle_{x=0} dt' \ . \tag{22}$$

For a square cross section, $\Upsilon_0 = \sigma_0 \Phi$ (see Sec. III A 1). The square and Lorentzian cases will now be discussed in detail.

1. Monochromatic radiation

In the case of a square cross section analytic solutions to the radiation transport equations can be obtained in closed form. From Eq. (19), we obtain the result

$$\frac{\partial \tau}{\partial t} = -\sigma_0 \phi_0(t)(1 - e^{-\tau}) \ , \tag{23}$$

where

$$\phi_0(t) = \int_0^\infty S_\nu(0,t) d\nu \approx S_0 \Delta\nu \ . \tag{24}$$

The last equality assumes S_ν is independent of ν in the bandwidth $\Delta\nu$. The same equations apply to the case of monochromatic radiation, provided we write the collimated monochromatic intensity as $S_\nu = S_0 \Delta\nu \delta(\nu - \nu_0)$. The solution of Eq. (23) is simply

$$e^{\tau} - 1 = (e^{\tau_0} - 1) \exp\left[- \int_0^t \sigma_0 \phi_0(t') dt' \right] \ , \tag{25}$$

where $\tau_0 = x/\zeta$. Substitution of Eq. (25) into Eq. (20) gives the results

$$\frac{n}{n_0} = \left[1 + \exp\left[- \frac{x - \Phi_0/n_0}{\zeta} \right] - \exp\left[- \frac{x}{\zeta} \right] \right]^{-1} \tag{26}$$

and

$$\exp(\sigma_0 \Phi) - 1 = \exp\left[- \frac{x}{\zeta} \right] [\exp(\sigma_0 \Phi_0) - 1] \ , \tag{27}$$

where the photon fluence $\Phi(t)$ is defined as

$$\Phi(t) = \int_0^t \phi(t') dt' \ . \tag{28}$$

This result was first derived by Bellman *et al.*,[1] and Frantz and Nodvik in 1963.[2] A similar calculation was reported by Ovchinnikov and Khartsiev[3] in 1965. The solutions give explicit expressions for $n(x,t)$ and $\Phi(x,t)$ in terms of $\Phi_0 = \Phi(x=0)$ and the optical depth ζ. In order to gain physical insight into these solutions we take $\Phi_0 = \phi_0 t$, define $v_b = \phi_0 / n_0$, and consider the behavior of Eq. (26) in the limit $x/\zeta \gg 1$ or $\sigma_0 \Phi_0 \gg 1$. Under these conditions, the fraction of absorbers removed by the radiation field can be written in the form

$$f_b \approx \left[1 + \exp\left[\frac{x - v_b t}{\zeta} \right] \right]^{-1} \ . \tag{29}$$

This represents a density wave driven by the radiation field that propagates with a velocity v_b and exhibits a constant shape wave front with a spatial thickness of the order of ζ. This wave is also re-

ferred to as a bleaching wave since the absorption behind the wave front is reduced by the radiation field. Retaining the time derivative in Eq. (A5), the exact expression for v_b is $\phi_0 c/(\phi_0+cn_0)$, so that in the limit of high intensity $v_b \to c$ as it should.

2. Broadband radiation

For broadband radiation, the frequency integration in Eq. (19) usually must be performed numerically for an arbitrary $g(\nu)$ and $S_\nu(0,t)$. If we assume that S_ν is slowly varying compared to $g(\nu)$, we can perform the change of variable $\Delta=2(\nu_0-\nu)/\Delta\nu$ and rewrite Eq. (19) in the approximate form

$$\frac{\partial\tau}{\partial t}\approx-\frac{\sigma_0\phi_0}{2}\int_{-\infty}^{\infty}\{1-\exp[-\tau g(\Delta)]\}d\Delta\ , \tag{30}$$

where $\Delta\nu$ is the full spectral width of the absorption feature. The solution of this equation is given implicitly by

$$\int_{\tau_0}^{\tau}\frac{d\tau'}{G(\tau')}=-\frac{\sigma_0\Phi_0(t)}{2}\ , \tag{31}$$

where

$$G(\tau)=\int_{-\infty}^{\infty}\{1-\exp[-\tau g(\Delta)]\}d\Delta\ . \tag{32}$$

Note that the total time dependence of $\tau(x,t)$ is determined by $\Phi_0(t)$.

If we now consider the example of a Lorentzian of the form $g(\Delta)=(1+\Delta^2)^{-1}$, the integral in Eq. (32) can be evaluated directly to the result

$$G(2\tau)=\pi\tau e^{-\tau}[I_0(\tau)+I_1(\tau)]\ , \tag{33}$$

where $I_n(\tau)$ is the nth order Bessel function. Substituting Eq. (33) into Eq. (31) gives the expression

$$\int_{\tau/2}^{\tau_0/2}\frac{e^y dy}{y[I_0(y)+I_1(y)]}=\frac{\pi}{2}\sigma_0\Phi_0(t)\ . \tag{34}$$

It is then expedient to numerically evaluate this integral and differentiate τ with respect to x to obtain $n(x,t)$. As indicated in Fig. 1, the wave fronts have constant shape and constant velocity only for a square cross section or monochromatic radiation.

We can easily demonstrate the physical behavior of the Lorentzian result in the limit that $\tau\gg1$. Using the asymptotic form of $I_n(\tau)\sim e^\tau/(2\pi\tau)^{1/2}$, the integral can be evaluated directly to give

$$\tau=\left[\tau_0^{1/2}-\frac{\sqrt{\pi}}{2}\sigma_0\Phi_0\right]^2\ , \tag{35}$$

which when substituted into Eq. (20) gives the result

$$f_b=\frac{1}{2}\left[\frac{\pi\zeta}{x}\right]^{1/2}\sigma_0\Phi_0(t)\ . \tag{36}$$

From the functional form of f_b, it is clear that the moving wave front does not exhibit a simple wave propagation solution. If we take a given point on the wave front, where f_b is constant and calculate an effective velocity $v_b'=dx/dt$, we obtain from Eq. (36) the value

$$v_b'=\frac{1}{f_b}\left[\frac{\pi x}{\zeta}\right]^{1/2}v_b\ , \tag{37}$$

where $v_b=\phi_0/n_0$ is the velocity of the bleaching wave for monochromatic radiation. The velocity of the front is different at each value of f_b and increases with x. Physically, this occurs because radiation in the far wings can propagate into the medium with the speed of light and produce nonlinear effects at a slow rate deep in the medium. These effects directly add to the wave-front behavior at the peak of the absorption feature as propagation proceeds. If we had retained the time-dependent term in the propagation equation, the limiting velocity would approach the velocity of light.

B. Noncollimated radiation

We now consider the effect of the angular dependence of I_ν on the radiation transport, first for a linear medium and then for a nonlinear one. Consider a medium at temperature T_m contained in an infinite slab of thickness d. Behind the slab is a blackbody radiation source at temperature T_e with a radiation intensity $I_{\nu e}(T_e)$ as shown in Fig. 2. We wish to calculate the intensity at the slab surface which is located at $x=0$. With the appropriate charge of variables in Eq. (A9) to fit the geometry of Fig. 2, the intensity is given by

$$I_\nu(\theta)=\int_0^{d/\cos\theta}\kappa_\nu I_{\nu e}(T_m)\exp\left[-\int_0^{s'}\kappa_\nu ds''\right]ds' +I_{\nu e}(T_e)\exp\left[-\int_0^{d/\cos\theta}\kappa_\nu ds''\right]\ . \tag{38}$$

If κ_ν and $I_{\nu e}$ are constant throughout the medium, the solution of Eq. (38) is

$$I_\nu(\theta)=I_{\nu e}(T_m)\left[1-\exp\left[-\frac{\tau_{\nu m}}{\cos\theta}\right]\right] +I_{\nu e}(T_e)\exp\left[-\frac{\tau_{\nu m}}{\cos\theta}\right]\ , \tag{39}$$

where $\tau_{\nu m}=\kappa_\nu d$ is the optical thickness along a perpendicular distance into the slab.

We now consider several situations of interest:

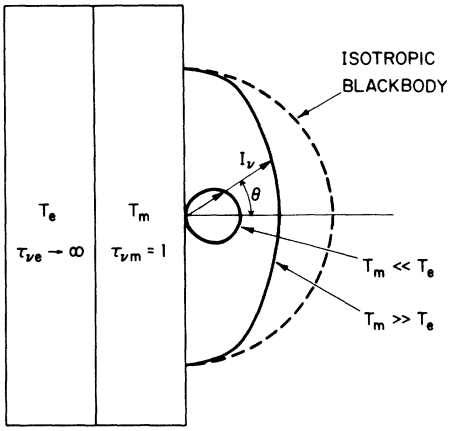

FIG. 2. Intensity distributions for radiation emitted from the surface of a slab of temperature T_m that is illuminated from the back surface by a blackbody source of temperature T_e. Optical thickness $\tau_{\nu m}$ of the slab here is unity.

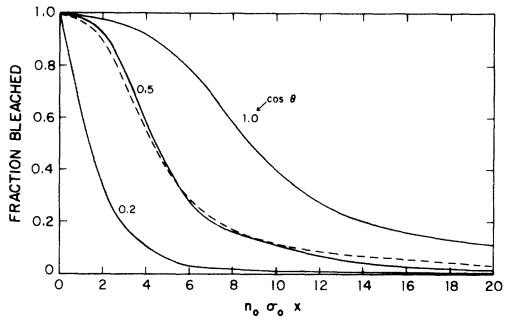

FIG. 3. Comparison of the bleaching waves in a Gaussian absorber obtained with isotropic radiation (dashed curve) and with collimated radiation incident at three different angles with respect to the normal to the slab ($\cos\theta = 1.0$, 0.5, and 0.2). Curves shown correspond to a time such that $\Upsilon_0 = 5$ [see Eq. (22)].

(i) $T_m \ll T_e$. If $\tau_{\nu m} \ll 1$, then $I_\nu(\theta) \approx I_{\nu e}(T_e)$ so that the radiation from the surface of the optically thin slab appears to be blackbody with a temperature T_e, both with respect to the angular and spectral distribution of the radiation. For $\tau_{\nu m} > 1$, the radiation near $\theta = 0$ appears to be blackbody; for larger values of θ, the radiation intensity is substantially less that of a blackbody. This behavior is shown schematically in Fig. 2.

(ii) $T_m \gg T_e$. If $\tau_{\nu m}/\cos\theta \ll 1$, then

$$I_\nu(\theta) \approx I_{\nu e}(T_m)\frac{\tau_{\nu m}}{\cos\theta} + I_{\nu e}(T_e) . \tag{40}$$

Under these conditions $I_\nu(\theta) \ll I_{\nu e}(T_m)$. For $\tau_{\nu m} > 1$, $I_\nu(\theta) \approx I_{\nu e}(T_m)[1 - \exp(-\tau_{\nu m}/\cos\theta)]$, which is also shown in Fig. 2. Under these conditions, the radiation is characterized by the medium and is not blackbody in the forward direction but approaches a blackbody distribution at some $\theta > 0$.

We finally consider a nonlinear medium with $T_m \ll T_e$. This is the situation of greatest interest for optical pumping. As a specific example we assume a Gaussian absorber and solve Eq. (12) numerically. The bleaching wave for isotropic irradiation of the slab is compared with the results of collimated radiation incident at three different angles in Fig. 3. The energy density at the surface $U_\nu(0,t)$ is the same in each case and the value of Υ_0, defined by Eq. (22), is 5.0 for the curves shown. The optical thickness to a given depth into the slab increases as the incident ray becomes more oblique. That is, penetration is deepest and consequently the bleaching wave front is most diffuse for normal incidence of collimated radiation.

The radiation from an emitting source of finite optical thickness $\tau_{\nu e}$ will also be anisotropic and, in addition, attenuated, viz.,

$$I_\nu(\theta) = I_{\nu e}(T_e)(1 - e^{-\tau_{\nu e}/\cos\theta}) . \tag{41}$$

Results for sources with four different optical thicknesses (for simplicity assumed to be independent of ν) are shown in Fig. 4. It can be observed that the effect of anisotropy is much greater than the effect of the reduction in integrated energy since the greatest loss, owing to the finite thickness of the source, occurs for the most penetrating normal rays.

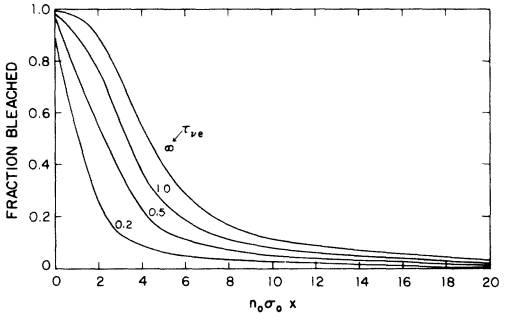

FIG. 4. Comparison of the bleaching waves in a Gaussian absorber pumped with radiation sources of various optical thicknesses ($\tau_{\nu e} = \infty$, 1.0, 0.5, and 0.2, as labeled). For $\tau_{\nu e} \to \infty$, $\Upsilon_0 = 5$.

IV. HYDRODYNAMIC DISTURBANCES IN THE MEDIUM

In certain situations involving radiative transfer, the medium behind the bleaching wave can be heated by the kinetic processes related to the interaction of radiation with the medium. In particular, photolysis and recombination lead to heat addition to the medium. This leads to a temperature and pressure gradient across the wave front. If the heat addition is sufficiently large, unsteady hydrodynamic disturbances can be radiated from the surface of the wave front. Under certain conditions, these disturbances can occur in the form of propagating shock waves that move ahead of the radiation front and modify the thermodynamic properties of the medium. These in turn modify the radiation transport. A correct description of the radiative transfer requires a self-consistent treatment of the hydrodynamics of the medium. We consider below a simplified analytical treatment to establish the change in the gas dynamic properties that occur across the wave front and the maximum heat addition that can occur in the medium before the onset of hydrodynamic disturbances in the flow.

A more general analysis of thermal waves has been reported by Ahlborn and Liese[20] using a similar analytic approach. We cast our results in a different representation, however, that provides broader physical insight into the hydrodynamic characteristics of the radiation driven wave front.

In this analysis, we assume that the radiation driven wave front propagates with a constant shape and at a constant velocity $D=\phi_0/n_0$. Behind the wave front, the various kinetic processes in the medium result in the addition of thermal energy q per unit mass of gas. For purposes of analysis, we consider this heat addition to occur over some well-defined volume immediately behind the front. If the propagation is assumed to be one dimensional, the wave front and local gas dynamic conditions are shown in Fig. 5. We now choose planes A and B in the upstream and downstream gas flow, respectively, that are sufficiently far removed from the wave front that the gas flow there is spatially uniform. The objective is to determine the gas density ρ, pressure P, internal energy ϵ, and gas flow velocity v at plane B in terms of the unperturbed values at plane A. The temperature of the gas is contained implicitly in $\epsilon(T)$. For the purposes of this analysis we consider the unperturbed gas to be stationary and we take v_0 to be zero.

Conservation of mass, momentum, and energy give the familiar Rankine-Hugoniot equations, which can be written in the form

$$\rho_1(D-v_1)=\rho_0 D\ , \tag{42}$$

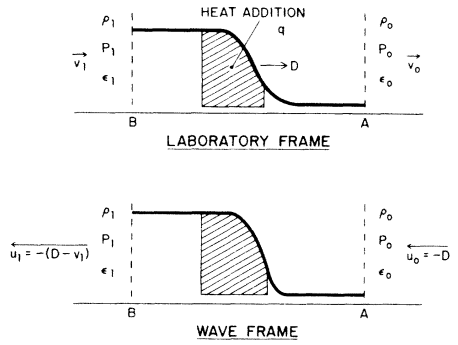

FIG. 5. Schematic diagram indicating the relationship of the gas dynamic variables in the laboratory and wave reference frames.

$$\rho_0 D v_1=P_1-P_0\ , \tag{43}$$

and

$$\rho_0 D\left[\epsilon_1-\epsilon_0+\frac{v_1^2}{2}\right]=P_1 v_1+q\ . \tag{44}$$

It is convenient to transform to the reference frame moving with the velocity of the radiation front. In this frame the wave front is stationary and the gas streams through the front with a velocity $u_0=-D$ and exits plane B with a velocity $u_1=-(D-v_1)$, as shown in Fig. 5. The conservation equations in this frame now become

$$\rho_1 u_1=\rho_0 u_0\ , \tag{45}$$

$$P_1+\rho_1 u_1^2=P_0+\rho_0 u_0^2\ , \tag{46}$$

and

$$\epsilon_1+\frac{P_1}{\rho_1}+\frac{u_1^2}{2}+q=\epsilon_0+\frac{P_0}{\rho_0}+\frac{u_0^2}{2}\ . \tag{47}$$

In addition, we must specify the equation of state of the gas which can be written in the functional form $P=P(\epsilon,\rho)$. Up to this point, the analysis is identical to that of the conventional propagation of a gas dynamic discontinuity in a gas. For the radiation-driven wave, however, the physical situation is quite different. The velocity of the wave front is constant and any gas dynamic disturbances or discontinuities are driven by the temperature discontinuity. In a shock wave the pressure gradient drives the shock forward and leads to discontinuities in the other flow variables. The shock velocity can adjust itself

to satisfy all three conservation equations over the complete range of the variables.

Usually the upstream conditions of the gas ρ_0, P_0, ϵ_0, and u_0 are known. We then have the three Rankine-Hugoniot equations plus the equation of state to determine the four equivalent downstream variables. If the equation of state and $\epsilon(T)$ are known, it is possible to obtain a solution for all of the unknown variables in terms of the heat addition q and the upstream conditions of the gas. Usually, this evaluation must be performed numerically.

In order to provide physical insight into the process, we consider the situation of an ideal gas for which $P=\rho RT$ and $\epsilon=C_vT$, where T is the temperature, C_v is the specific heat at constant volume, and R is the gas constant. It is convenient to eliminate R and normalize all velocities to the local sound speed in the gas c_0 through the relation

$$c_0^2=\gamma RT=\gamma P/\rho\ , \tag{48}$$

where $\gamma=C_p/C_v$, the ratio of specific heats at constant pressure and volume. The internal energy is now given by the relation $\epsilon=(\gamma-1)^{-1}P/\rho$. In analogy with conventional gas dynamic discontinuities, we also define a local Mach number $M=u/c_0$. We will also consider a "Mach number" for the radiation front $M_0=D/c_0$ even though there is no gas dynamic motion.

From the continuity and momentum equations we obtain

$$u_1=\frac{\rho_0u_0^2-(P_1-P_0)}{\rho_0u_0}\ . \tag{49}$$

From this relation it is clear that $\rho_0u_0^2>(P_1-P_0)$ for steady-state flow, which is a simple statement that the dynamic pressure of the flow $\rho_0u_0^2$ must exceed the pressure gradient across the discontinuity. If this is not the case, steady-state flow does not obtain with a single discontinuity. In a simple gas dynamic situation with no heat addition, the velocity of the discontinuity adjusts itself to ensure that this condition is always satisfied. With radiation driven waves u_0 is fixed and (P_1-P_0) is determined by the heat addition. Consequently, a transition to unsteady flow occurs when $u_1=0$. We will return to this point.

The remainder of the analysis parallels that of Ref. 21. The effect of heat addition to the flow is best measured in terms of the *total* energy in the upstream flow q_0, where

$$q_0=C_pT_0+\frac{u_0^2}{2}\ . \tag{50}$$

Using Eqs. (45)—(48) we obtain the result that

$$\bar{q}=\frac{q}{q_0}+1=\frac{M_1^2}{M_0^2}\left[\frac{1+\gamma M_0^2}{1+\gamma M_1^2}\right]^2\left[\frac{1+\frac{\gamma-1}{2}M_1^2}{1+\frac{\gamma-1}{2}M_0^2}\right]\ , \tag{51}$$

where $1\le\bar{q}<\infty$. A plot of Eq. (51) is shown in Fig. 6. The solutions indicated by the dotted curves are not allowed because of entropy considerations. It is clear from the physical situation that for $\bar{q}=1$ there are no gas dynamic discontinuities and the solution is confined to the line $M_1=M_0$. As $\bar{q}$ increases, all other solutions are allowed. For $M_0>1$ and $\bar{q}\gtrsim1$, the functional form for M_1 is double valued. Initially, the solution is confined to the curve for which $M_1>1$. As $\bar{q}$ increases, any formation of compression waves in the medium can effect a transition to the compression shock curve for which $M_1<1$. However, this requires a finite formation time to establish a steady-state flow. From this figure it is clear that for any given value of M_0, $\bar{q}$ can increase until $M_1=1$. At this critical value $\bar{q}_m$, the flow becomes unstable.

The dependence of $\bar{q}_m$ on M_0 can be determined from Eq. (51) by setting $M_1=1$. It is more convenient, however, to compare the value of q_m with the internal energy C_pT_0 in the upstream flow, since q_0 varies with M_0. From Eq. (50) and the definition of q_0, one can derive the relation

$$\frac{q_m}{C_pT_0}=\frac{T_m}{T_0}-1=\frac{1}{2(\gamma+1)}\frac{(M_0^2-1)^2}{M_0^2}\ . \tag{52}$$

A plot of q_m/C_pT_0 for $\gamma=1.4$ is shown in Fig. 7. As is well known, the net effect of increasing q at a constant M_0 is to accelerate the gas if $M_0<1$ and decelerate the gas if $M_0>1$.

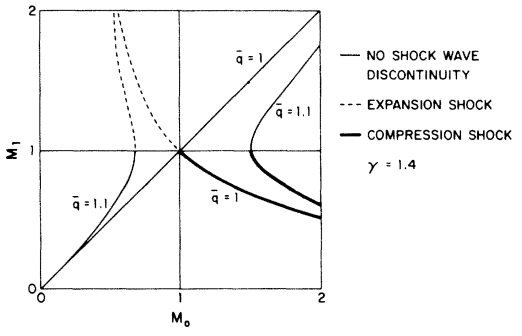

FIG. 6. Plot of the Mach number M_1 behind the wave front as a function of the wave Mach number M_0 for various types of gas dynamic discontinuities.

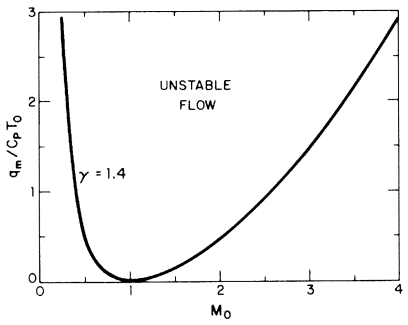

FIG. 7. Maximum stable heat addition to the flow (normalized to the thermal energy in the medium) as a function of the velocity (Mach number) of the wave front. Unstable flow obtains in the parameter space above the curve.

The use of Eqs. (45)–(48) leads to the following relations for the downstream gas:

$$\frac{T_1}{T_0}=\frac{M_1^2}{M_0^2}\left[\frac{1+\gamma M_0^2}{1+\gamma M_1^2}\right]^2, \tag{53}$$

$$\frac{P_1}{P_0}=\frac{1+\gamma M_0^2}{1+\gamma M_1^2}, \tag{54}$$

and

$$\frac{\rho_1}{\rho_0}=\frac{M_0^2}{M_1^2}\left[\frac{1+\gamma M_1^2}{1+\gamma M_0^2}\right]=\frac{u_0}{u_1}. \tag{55}$$

For given values of q and M_0, M_1 is uniquely determined from Eq. (51). Substitution of M_0 and M_1 into the above equations yields the values of T_1, P_1, ρ_1, and u_1. The maximum values of these variables are obtained by setting $M_1^2=1$.

We note that for large velocities of the bleaching wave ($M_0^2 \gg 1$), the temperature and pressure increases are large, but the density change is small and simply accommodates the change in material velocity to assure conservation of mass. In the limit of large M_0^2, $\rho_1/\rho_0=(1+\gamma)/\gamma$. Consequently, it is a good assumption to neglect the number-density variations resulting from hydrodynamic effects in calculating the kinetic processes behind the radiation front when $M_0^2 > 1$. This is not the case if $M_0^2 \ll 1$.

If $q \geq q_m$, $M_1=1$. In order to satisfy the conservation laws, additional pressure waves will be generated to decrease the value of M_0. In a gas dynamic flow this condition is referred to as "choked flow." If M_0 is supersonic, additional shocks will be established upstream to decrease the value of M_0 to a subsonic value. This situation differs from a Chapman-Jouguet detonation where the heat addition owing to the chemical reaction drives M_1 to unity but adjusts the detonation velocity of the shock front to give the appropriate value of M_0.

If $M_0 \approx 1$, even a small heat addition to the gas can lead to hydrodynamic disturbances emanating from the radiation driven wave front. For example, for $M_0^2=2$ and $\gamma=1.4$, $T_m/T_0 \approx 1.1$. Therefore, a 10% increase in the gas temperature is sufficient to generate unstable hydrodynamic disturbances in the flow under these conditions. However, for most applications of interest, the radiation intensity is sufficiently large that the bleaching wave velocity is much greater than the speed of sound in the medium. Typically $M_0 > 10$ and Eq. (52) goes over to the limit

$$\frac{q_m}{C_pT_0}=\frac{T_m}{T_0}-1 \approx \frac{1}{2(\gamma+1)}M_0^2. \tag{56}$$

Consequently, unstable hydrodynamic disturbances will not form under these conditions.

The above analysis is based on the assumption of steady-state flow. A more accurate evaluation of hydrodynamic effects involves the consideration of the time-dependent evolution of the disturbance under the conditions of unsteady flow. If the velocity of the bleaching wave is sufficiently large such that $M_0 \gg 1$, a temperature and pressure discontinuity will occur in the medium, but a finite time is required to establish a density discontinuity and conditions of steady state. Also time-dependent hydrodynamic disturbance can occur for any finite value of $\bar{q}$ if $M_0 < 1$.

A time-dependent analysis has been performed by Ishii and Ahlborn[22] for radiation transport in an atomic iodine laser. The parent iodine-containing molecule acts as an absorber for ultraviolet (uv) radiation from an optical pumping source. The molecule dissociates with time in the presence of the radiation field to produce an inverted population of iodine atoms for the laser. Depending on the intensity, the uv radiation may simply attenuate in the absorbing medium or can propagate into the medium as a bleaching wave. Their analysis assumed a monochromatic pump source. The results indicate three different operating regimes can occur: (a) a subsonic mode $M_0 < 1$ in which the heat addition due to photolysis drives a supersonic shock wave ahead of the photolysis wave, (b) a supersonic mode $M_0 > 1$ in which the absorption or photolysis front propagates faster than the local sound speed so that no shock or any hydrodynamic disturbance can develop ahead of the radiation wave front, and (c) a Chapman-Jouguet mode where the shock wave is attached to the absorption front.

These results are in qualitative agreement with the steady-state analysis presented above. The supersonic mode (b) corresponds to the supersonic curve in Fig. 6 for which $M_0>1$ and $M_1>1$. The Chapman-Jouguet mode corresponds to the compression shock curve for which $M_0>1$ and $M_1<1$. The subsonic mode is a nonsteady solution that is derived from the subsonic curve in Fig. 6 but cannot be predicted by a strict steady-state flow analysis. This problem has also been addressed numerically in our laboratory using a fully time-dependent two-dimensional hydrodynamic calculation. The results indicate that the use of a steady-state flow analysis with adiabatic heat addition is an excellent approximation for most conditions of interest. Even in the subsonic regime, the system achieves a new steady state after a few acoustic transit times that only differs slightly from that predicted by the previous analysis.

The assumption of a monochromatic pump source for the iodine laser may not be a good approximation for a quantitative description of the propagation of the bleaching wave. Other effects such as chemical kinetic processes in the medium also strongly influence the behavior of the bleaching wave. A detailed analysis of the iodine laser, including the effects of a broadband optical pump source and the medium kinetics, will be considered in a separate paper.

ACKNOWLEDGMENTS

The authors gratefully acknowledge many beneficial discussions with T. P. Cotter, J. T. Lee, and W. C. Davis. The time-dependent hydrodynamic calculations were performed by M. Klein and J. Hyde, and contributed greatly to our understanding of this area. This work was performed under the auspices of the U.S. Department of Energy.

APPENDIX: LINEAR RADIATION TRANSPORT

In this appendix, we review the derivation of the equations for radiation transport in a linear medium.[23,24] The results used to describe nonlinear radiation transport are similar. The radiation field can be described in terms of a scalar photon spectral intensity function $I_\nu(\vec{r},t,\hat{\Omega})$, where $I_\nu d\nu d\Omega$ is the number of photons at time t in a frequency range ν to $\nu+d\nu$ passing per unit of time through a unit area located at position $\vec{r}$ and contained within a solid angle $d\Omega$ in a direction of a unit propagation vector $\hat{\Omega}$. The emitting area is normal to $\hat{\Omega}$. The subscript ν designates a spectral quantity. The spectral photon density $U_\nu(\vec{r},t)$ is then

$$U_\nu(\vec{r},t)=\frac{1}{c}\int_{4\pi} I_\nu d\Omega \ . \tag{A1}$$

Now consider the propagation of photons through a plane with a normal $\hat{n}$ that makes an angle θ to $\hat{\Omega}$. The vector photon flux $\vec{S}_\nu(\vec{r},t)$ is given by

$$\vec{S}_\nu(\vec{r},t)=\int_{4\pi} I_\nu(\vec{r},t,\hat{\Omega})\hat{\Omega}\, d\Omega \ . \tag{A2}$$

The scalar component of the photon flux along the normal is $\hat{n}\cdot\vec{S}_\nu$, which can be written in the form

$$S_\nu(\vec{r},t,\hat{n})=\int_{4\pi} I_\nu(\vec{r},t,\hat{\Omega})\cos\theta\, d\Omega \ . \tag{A3}$$

From this definition, the value of S_ν depends on the orientation of the surface, i.e., $\hat{n}$.

Consider the transport of radiation along a path that is aligned in the direction of $\hat{\Omega}$. Conservation of photons requires that I_ν satisfy the equation

$$\frac{1}{c}\frac{\partial I_\nu}{\partial t}+\hat{\Omega}\cdot\vec{\nabla} I_\nu=\Delta_\nu \ , \tag{A4}$$

where Δ_ν is the net gain in the number of photons over the losses. The photon losses are due to absorption while the photon sources are due to stimulated and spontaneous emission processes. The absorption in the medium can be characterized by an absorption coefficient $\kappa'_\nu(\vec{r},t)$ which depends on the number of molecules in the absorbing state. It is also possible to include the effects of stimulated emission by defining a net absorption coefficient $\kappa_\nu(\vec{r},t)$ which now depends on the population density in the upper state as well as the lower state. Since these population densities in general depend on I_ν, the value of κ_ν is also an implicit function of I_ν. For spontaneous emission, we define a spectral intensity $I_{\nu e}$ which can be related to the absorption of the medium by Kirchoff's radiation laws. The result is that the net absorption in the medium can be reduced to a term of the form $\kappa_\nu(I_\nu-I_{\nu e})$. Equation (A4) may now be written in the form

$$\frac{1}{c}\frac{\partial I_\nu}{\partial t}+\hat{\Omega}\cdot\vec{\nabla} I_\nu=-\kappa_\nu(\vec{r},t)(I_\nu-I_{\nu e}) \ . \tag{A5}$$

A continuity equation for the radiation field can be obtained by integrating Eq. (A5) over all directions $\hat{\Omega}$. Using the definition of U_ν and $\vec{S}_\nu$ we obtain the result

$$\frac{\partial U_\nu}{\partial t}+\vec{\nabla}\cdot\vec{S}_\nu=-c\kappa_\nu(\vec{r},t)(U_\nu-U_{\nu e}) \ . \tag{A6}$$

A useful solution of Eq. (A5) can be obtained as

follows. We consider a propagation path of the radiation along a coordinate s so that $\vec{\nabla}\rightarrow\partial/\partial s$. A simple transformation to the retarded time $t'=t-s/c$ in Eq. (A5) results in an equation of the form

$$\frac{\partial I_\nu}{\partial s}=-\kappa_\nu(s,t'+s/c)(I_\nu-I_{\nu e})\ . \tag{A7}$$

When integrated and transformed back to the original coordinates Eq. (A7) has the formal solution

$$I_\nu(s,t)=I_\nu\left[s_0,t-\frac{s-s_0}{c}\right]\exp\left[-\int_{s_0}^{s}\kappa_\nu\left[s'',t-\frac{s-s''}{c}\right]ds''\right]$$
$$+\int_{s_0}^{s}\kappa_\nu\left[s',t-\frac{s-s'}{c}\right]I_{\nu s}\left[s',t-\frac{s-s'}{c}\right]\exp\left[-\int_{s'}^{s}\kappa_\nu\left[s'',t-\frac{s-s''}{c}\right]ds''\right]ds'\ , \tag{A8}$$

where s_0 is the coordinate of the photon source. In many cases of interest, the propagation time over the length of the medium is short compared to the time scale for changes in the source or in the medium. We see from Eq. (A8) that this condition is formally equivalent to allowing c to approach infinity in Eq. (A7). Although the time-derivative term is important for temporal changes in a propagating pulse, in most of the discussion related to present applications, we can neglect the finite propagation time of the radiation. The radiation field can then be written in the form

$$I_\nu(s,t)=I_\nu(s_0,t)\exp\left[-\int_{s_0}^{s}\kappa_\nu(s'',t)ds''\right]+\int_{s_0}^{s}\kappa_\nu(s',t)I_{\nu s}(s',t)\exp\left[-\int_{s'}^{s}\kappa_\nu(s'',t)ds''\right]ds'\ . \tag{A9}$$

These results are applied to radiation transport in one dimension. The only modification required for nonlinear radiation transport is that κ_ν may be an implicit function of I_ν. In linear radiation transport, the solutions of the transport equations can be obtained for each spectral component I_ν, S_ν, and U_ν. For nonlinear radiation transport, the solution will contain frequency-convoluted terms involving κ_ν and I_ν.

[1]R. Bellman, G. Birnbaum, and W. G. Wagner, J. Appl. Phys. 34, 780 (1963).

[2]L. M. Frantz and J. S. Nodvik, J. Appl. Phys. 34, 2346 (1963).

[3]V. M. Ovchinnikov and V. E. Khartsiev, Zh. Eksp. Teor. Fiz. 49, 315 (1965) [Sov. Phys.—JETP 22, 221 (1966)].

[4]B. L. Borovich, V. S. Zuev, V. A. Katulin, O. Yu. Nosach, E. L. Tyurin, and V. A. Shcheglov, Kvant. Elektron. (Moscow) 2, 88 (1972) [Sov. J. Quantum Electron. 2, 160 (1972)].

[5]B. L. Borovich, V. Ya. Karpov, N. I. Kozlov, and Yu. Yu. Stoilov, Zh. Eksp. Teor. Fiz. 64, 1211 (1973) [Sov. Phys.—JETP 37, 616 (1973)].

[6]B. L. Borovich, V. S. Zuev, and O. N. Krokhin, Zh. Eksp. Teor. Fiz. 64, 1184 (1973) [Sov. Phys.—JETP 37, 602 (1973)].

[7]V. E. Khartsiev, Zh. Tekh. Fiz. 47, 2444 (1977) [Sov. Phys. Tech. Phys. 22, 1418 (1977)].

[8]A. A. Makarov, C. D. Cantrell, and W. H. Louisell, Opt. Commun. 31, 31 (1979).

[9]C. D. Cantrell, A. A. Makarov, and W. H. Louisell, in *Photoselective Chemistry*, edited by J. Jortner, R. D. Levine, and S. A. Rice (Wiley, New York, 1981), pp. 583–624.

[10]J. H. Eberly, M. J. Konopnicki, and B. W. Shore, Opt. Commun. 35, 76 (1980).

[11]C. D. Cantrell, F. Rebentrost, and W. H. Louisell, Opt. Commun. 36, 303 (1981).

[12]M. T. Sandford, R. W. Whitaker, and R. I. Klein, Astrophys. J. 260, 183 (1982).

[13]J. Zinn and R. C. Anderson, Phys. Fluids 16, 1639 (1973); J. Zinn and C. D. Sutherland, Los Alamos National Laboratory Report LA-UR-81-1893 (unpublished).

[14]V. E. Khartsiev, Zh. Eksp. Teor. Fiz. 54, 867 (1968) [Sov. Phys.—JETP 27, 464 (1968)].

[15]V. Yu. Zalesskii, Zh. Eksp. Teor. Fiz. 69, 513 (1975) [Sov. Phys.—JETP 42, 262 (1975)].
[16]G. A. Skorobogatov, Pis'ma Zh. Tekh. Fiz. 1, 452 (1975) [Sov. Tech. Phys. Lett. 1, 209 (1975)].
[17]G. N. Vinokurov and V. Yu. Zalesskii, Kvant. Electron. (Moscow) 5, 2110 (1978) [Sov. J. Quantum Electron. 8, 1191 (1978)].
[18]G. N. Vinokurov, V. Yu. Zalesskii, and P. I. Krepostnov, Kvant. Elektron. (Moscow) 7, 944 (1980) [Sov. J. Quantum Electron. 10, 539 (1980)].
[19]I. A. Izmailov and V. A. Kochelap, Kvant. Elektron. (Moscow) 6, 2349 (1979) [Sov. J. Quantum Electron. 9, 1383 (1979)].
[20]B. Ahlborn and W. Liese, Phys. Fluids 24, 1955 (1981).
[21]A. H. Shapiro, *Dynamics and Thermodynamics of Compressible Fluid Flow* (Ronald, New York, 1953), Vol. 1, Chap. 6.
[22]S. Ishii and B. Ahlborn, J. Appl. Phys. 47, 1076 (1976).
[23]Ya. B. Zel'dovich and Yu. P. Raizer, *Physics of Shock Waves and High Temperature Hydrodynamic Phenomena* (Academic, New York, 1966), Vol. 1, Chap. II.
[24]S. Chandrasekhar, *Radiative Transfer* (Dover, New York, 1960).